The Journal of Chemical Physics

Vibrational quenching of CN^- in collisions with He and Ar

Cite as: J. Chem. Phys. **154**, 084305 (2021); https://doi.org/10.1063/5.0039854
Submitted: 07 December 2020 . Accepted: 18 January 2021 . Published Online: 23 February 2021

Barry Mant, Ersin Yurtsever, Lola González-Sánchez, Roland Wester, and Franco A. Gianturco

The Journal of Chemical Physics ARTICLE scitation.org/journal/jcp

Vibrational quenching of CN^- in collisions with He and Ar

Cite as: J. Chem. Phys. 154, 084305 (2021); doi: 10.1063/5.0039854
Submitted: 7 December 2020 • Accepted: 18 January 2021 •
Published Online: 23 February 2021

Barry Mant,[1] Ersin Yurtsever,[2] Lola González-Sánchez,[3] Roland Wester,[1] and Franco A. Gianturco[1,a)]

AFFILIATIONS

[1] Institut für Ionenphysik und Angewandte Physik, Universität Innsbruck, Technikerstr. 25/3, 6020 Innsbruck, Austria
[2] Department of Chemistry, Koç University, Rumelifeneri yolu, Sariyer, TR-34450 Istanbul, Turkey
[3] Departamento de Química Física, University of Salamanca, Plaza de los Caídos sn, 37008 Salamanca, Spain

Note: This paper is part of the JCP Special Topic on Quantum Dynamics with *Ab Initio* Potentials.
[a)] **Author to whom correspondence should be addressed:** francesco.gianturco@uibk.ac.at

ABSTRACT

The vibrational quenching cross sections and corresponding low-temperature rate constants for the $v = 1$ and $v = 2$ states of $CN^-(^1\Sigma^+)$ colliding with He and Ar atoms have been computed *ab initio* using new three-dimensional potential energy surfaces. Little work has been carried out so far on low-energy vibrationally inelastic collisions for anions with neutral atoms. The cross sections and rates calculated at energies and temperatures relevant for both ion traps and astrochemical modeling are found by the present calculations to be even smaller than those of the similar C_2^-/He and C_2^-/Ar systems, which are in turn of the order of those existing for the collisions involving neutral diatom–atom systems. The implications of our finding in the present case mainly focus on the possible role of small computed rate constants in the dynamics of molecular cooling and the evolution of astrochemical modeling networks.

I. INTRODUCTION

Vibrationally inelastic collisions are fundamental processes in chemical physics and molecular dynamics. Gas phase collisions, which can excite or quench a vibrational mode in a molecule, have been studied both experimentally and theoretically for decades[1–5] and are generally well understood. Typically, the scattering cross sections and corresponding rates are relatively small[6] due to the generally large energy spacing between vibrational levels that require strong interaction forces between the colliding species to induce transitions. On the other hand, these processes still attract a great deal of attention and study as they have important applications in fields such as cold molecules, where collisions are used to quench internal molecular motion,[7–9] or astrochemistry, where accurate rate constants are necessary to model the evolution of gas clouds and atmospheres.[10–14] There are also exceptional systems such as the dramatic case of $BaCl^+$ + Ca where laser cooled calcium atoms can efficiently quench vibrational motion with rates similar to rotational transitions.[9,15]

There continue to be many studies of diatom–atom vibrationally inelastic collisions for both neutral[7,11,16,17] and cationic species.[15,18–20] This is to be contrasted with the case for anions, where very little work has been carried out on vibrationally inelastic collision processes. Recently, we have tried to change this trend and have investigated vibrational quenching of the C_2^- anion in collisions with noble gas atoms.[21] This molecule is of direct interest as a possible candidate for laser cooling mechanisms,[22] but a first step will require the cooling of internal motion via collisions since spontaneous dipole emission is forbidden for the rovibrational excited states of this homonuclear species. The cross sections and rate constants for vibrational transitions were found by our calculations to be small, i.e., of the order of those for neutral species.

In this article, we report the vibrational quenching of yet another important anion, CN^-, in collisions with He and Ar atoms. The cyanide anion is a well studied molecule, particularly its spectroscopic properties have attracted a great deal of attention and investigations[23–28] as well as the determination of its photodetachment energy.[23,29,30] Recent work in our group has further clarified

important aspects of its photodetachment behavior at the threshold from cold trap experiments.[31] This molecule has also been detected in the envelope of a carbon star[32] after its rotational constants were carefully measured.[25] Collisional processes of the anion with the astrochemically relevant He and H_2 species[33,34] for rotational transitions have recently been studied and we have also investigated the rotational cooling of this molecular anion with He, Ar, and H_2 as buffer gasses.[35] The CN^- anion is also thought to be an important participant as well in reactions in the interstellar medium (ISM)[36–39] and in the atmosphere of Titan[40] where it has been detected.[41,42]

We note in passing that the corresponding neutral species CN was one of the first molecules to be detected in space[43] and cross sections and rates for this species have been investigated and obtained for various rovibrational process in collisions with He and H_2.[16,44–49] The cyanide cation is also suspected to be important to astrochemical processes but has yet to be detected. The cation's vibrational energies have recently been measured[50] as well as a study has been carried out on its rotational transitions induced by He collisions.[51]

Vibrationally inelastic collisions involving the CN^- molecular anion with neutral atoms are a type of process rarely studied for such systems. Although CN^- can, in fact, lose energy through spontaneous emission, its wide relevance justifies providing an accurate assessment of the vibrational quenching processes involving He and Ar, typical buffer gasses in ion traps.

This paper is organized as follows: Sec. II presents the CN^- potential energy and dipole moment curves (DMCs) along with the anion's vibrational energy levels and Einstein A coefficients. The potential energy surfaces (PESs) for the CN^-/He and CN^-/Ar systems are then discussed in Sec. III. The quantum scattering methodology is described in Sec. IV and scattering cross sections and rates are discussed in Sec. V. Conclusions are given in Sec. VI.

II. CN^- POTENTIAL ENERGY CURVE AND DIPOLE MOMENT

Electronic energies for the ground $^1\Sigma^+$ state of the CN^- anion were calculated at 19 internuclear distances r to obtain the anion's potential energy curve (PEC). Calculations were carried out using the MOLPRO suite of quantum chemistry codes[52,53] at the coupled-cluster-single-double-and-perturbative-triple [CCSD(T)] level of theory[54,55] employing an aug-cc-pV5Z basis set.[56,57] The expectation value of the non-relaxed CCSD dipole moment at each r distance was also obtained. The *ab initio* energies and dipole moment curve (DMC) for CN^- are shown in Fig. 1.

The LEVEL program[58] was used to obtain the vibrational energies and wavefunctions for the CN^- molecule. The *ab initio* energies were used as an input, interpolated using a cubic spline and extrapolated to r values below and above the range of calculated energies using functions implemented in LEVEL. The relative energies of the first three vibrational levels along with the rotational constants for each state are shown in Table I and compared with previously published calculated theoretical and experimental values. The agreement with previous calculations and experimental values is quite good and certainly sufficient to evaluate the cross sections and rate constants of inelastic collisions considered below.

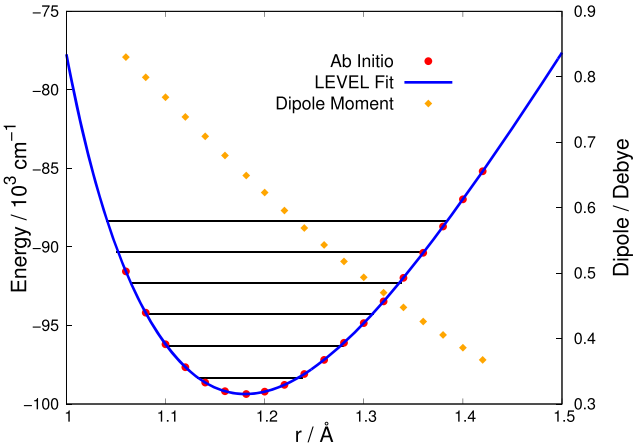

FIG. 1. *Ab initio* energies, PEC fit, and DMC for CN^- ($^1\Sigma^+$). The horizontal lines show the first six vibrational energies.

We have recently evaluated the dipole moment of CN^- at its equilibrium bond length r_{eq} using a variety of *ab initio* methods and basis sets[33] and used it to evaluate the Einstein A coefficients for pure rotational transitions. The best estimate of that work of 0.71 D is in quite good agreement with the value of the DMC at r_e of 0.65 D computed here. The LEVEL program was also used to calculate the Einstein A coefficients for rovibrational transitions of CN^- using the *ab initio* calculated DMC. The values of $A_{v'j',v''j''}$ for the first two vibrational states of the anion are shown in Table II and compared to those of neutral CN.[59] The values for the anion and neutral molecule are broadly similar, which is reasonable considering they have very similar bond lengths and vibrational energies.[59] The slightly larger values for neutral CN are a result of the larger dipole moment for the neutral molecule.[59]

TABLE I. Comparison of vibrational energies and rotational constants with previous theoretical and experimental values. Literature values calculated from Dunham parameters are provided. Units in cm^{-1}.

		Relative energy	B_v
v_0	This work	0	1.864
	Calc.[28]	0	1.868
	Expt.[25]	0	1.872
v_1	This work	2040	1.845
	Calc.[28]	2045	1.851
	Expt.[23]	2035 (±40)	
	Expt.[24]	2053 (neon)	
v_2	This work	4055	1.831
	Calc.[28]	4065	1.834

TABLE II. Einstein A coefficients $A_{v',v''}$ for selected CN^- ($^1\Sigma^+$) vibrational transitions compared to those for neutral CN ($^2\Sigma^+$) calculated by Brooke *et al.*[59] For CN^-, the P(1) branch values were used to compare to the Q-branch values for CN. Units in s^{-1}.

Transition	CN^-	CN
$v_1 \rightarrow v_0$	6.60	8.85
$v_2 \rightarrow v_1$	12.50	16.50
$v_2 \rightarrow v_0$	0.36	0.66

III. CN^-/He AND CN^-/Ar POTENTIAL ENERGY SURFACES AND VIBRATIONALLY AVERAGED MATRIX ELEMENTS

The interaction energies between CN^- in its ground $^1\Sigma^+$ electronic state with He and Ar atoms were calculated using *ab initio* methods implemented in the MOLPRO suite of codes.[52,53] Geometries were defined on a Jacobi grid with R (the distance from the center of mass of CN^- to the atom) ranging from 2.5 to 20 Å and θ (the angle between R and the CN^- internuclear axis r) from 0 (C side) to 180° in 15° and 10° intervals for He and Ar, respectively. Seven values of the CN^- bond length for each system between r = 1.00 Å–1.42 Å were used including the equilibrium value of r_{eq} = 1.181 431 Å. This is sufficient to cover the vibrational levels of interest in the present study. Interaction potential energies between CN^- and the noble gas atoms were determined by subtracting the asymptotic energies for each bond length.

For CN^-/He, energies were calculated using the multiconfigurational self-consistent field (MCSCF) method[60,61] with eight occupied orbitals and two closed orbitals followed by a one-state multi-reference configuration interaction (MRCI)[62] calculation. An aug-cc-pV5Z basis[63] was employed. In our earlier discussion of the CN-/He PES,[33] we discuss, in detail, the reasons why we followed both methods for this system and compared the CASSCF + MRCI results with the CCSD(T) with similar basis set expansions, finding them to be coincident in values. In particular, we corrected for the size-consistency possible shortcomings of the CASSCF + MRCI vs the CCSD(T) methods by correcting the former results using the Davidson's correction as implemented in MOLPRO. In our earlier work,[33] we showed that this correction brought the two sets of potential calculations to yield the same potential values over a broad range of the employed grid. As an example, we note here that from our CBS (Complete Basis Set) extrapolated CCSD(T) calculations on the CN^-/He system, we find the minimum energy configuration as theta = 40° and R = 3.95 Å with basis-set-superposition-error (BSSE) corrected energy at 49.522 cm^{-1}. CBS is calculated by the default procedure in MOLPRO: it is the so-called L3 extrapolation discussed in our earlier study. The results within the CAS(8,4) within the CASSCF + MRCI gave a theta = 40°, R = 4.00, and an energy of 50.39 cm^{-1} for its minimum configuration, showing the two methods to provide essentially the same results.

For the CN^-/Ar system, energies were calculated using the CCSD(T) method[55] with complete basis set (CBS) extrapolation using the aug-cc-pVTZ, aug-cc-pVQZ, and aug-cc-pV5Z basis sets.[56,64] The basis-set-superposition-error (BSSE) was also accounted for all calculated points using the counterpoise procedure.[65]

The three-dimensional PESs were fit to an analytical form using the method of Werner, Follmeg, and Alexander,[11,66] where the interaction energy is given as

$$V_{\rm int}(R,r,\theta) = \sum_{n=0}^{N_r-1}\sum_{l=0}^{N_\theta-1} P_l(\cos\theta)A_{ln}(R)(r-r_{eq})^n, \tag{1}$$

where $N_r = 7$ and $N_\theta = 13$ or 19, respectively, are the number of bond lengths r and angles θ in the *ab initio* grid, $P_l(\cos\theta)$ are the Legendre polynomials and r_{eq} = 1.181 431 Å is the equilibrium bond length of CN^-. For each bond length r_m and angle θ_k, one-dimensional cuts of the PESs $V_{\rm int}(R, r_m, \theta_k)$ were fit to

$$B_{km}(R) = \exp(-a_{km}R)\left[\sum_{i=0}^{i_{\max}} b_{km}^{(i)}R^i\right] - \frac{1}{2}[1+\tanh(R)]\left[\sum_{j=j_{\min}}^{j=j_{\max}} c_{km}^{j}R^{-j}\right], \tag{2}$$

where the first terms account for the short range part of the potential and the second part for the long range terms combined using the $\frac{1}{2}[1+\tanh(R)]$ switching function. For each r_m and θ_k, Eq. (2) was least squares fit to the *ab initio* data (around 40 R points) using $i_{\max} = 2$, $j_{\min} = 4$, and $j_{\max} = 10$ for eight variable parameters. The average root-mean-square error (RMSE) for each fit was 0.21 cm^{-1} for CN^-/He and 0.27 cm^{-1} for CN^-/Ar. From the 1D potential fits $B_{km}(R)$, the radial coefficients $A_{ln}(R)$ can be determined from the matrix product $\mathbf{A}(R) = \mathbf{P}^{-1}\mathbf{B}(R)\mathbf{S}^{-1}$, where the matrix elements of $\mathbf{P}$ and $\mathbf{S}$ are given as $P_{kl} = P_l(\cos\theta_k)$ and $S_{nm} = (r_m - r_{eq})^n$, respectively. The analytical representation of the PES, Eq. (1), gives a reasonable representation of the *ab initio* interaction energies. An overall RMSE of 82 cm^{-1} for all points used in the fit was obtained for CN^-/He, but this drops to 0.26 cm^{-1} for $V < 500$ cm^{-1}. For CN^-/Ar, an overall RMSE of 21 cm^{-1} was obtained, a value which went down to 1.5 cm^{-1} for $V < 500$ cm^{-1}.

The scattering calculations described in Sec. IV require the interaction potential to be averaged over the vibrational states of CN^- $\chi_v(r)$, which were obtained from LEVEL as described in Sec. II, as

$$V_{v,v'}(R,\theta) = \langle\chi_v(r)|V_{\rm int}(R,r,\theta)|\chi_{v'}(r)\rangle. \tag{3}$$

Figure 2 shows the diagonal terms $V_{0,0}(R, \theta)$ for both systems. As expected for a molecule with a strong bond, so that the ground state vibrational wavefunction is strongly peaked around r_{eq}, the contour plots of the $V_{0,0}(R, \theta)$ for each system are very similar to our earlier rigid-rotor (RR) PESs that were obtained without the vibrational averaging.[33,35] PESs of both systems have a fairly similar appearance with the most attractive part of the potential located on the nitrogen end of CN^-. The well depth is the main difference, which increases as expected from He to Ar due to the increasing number of

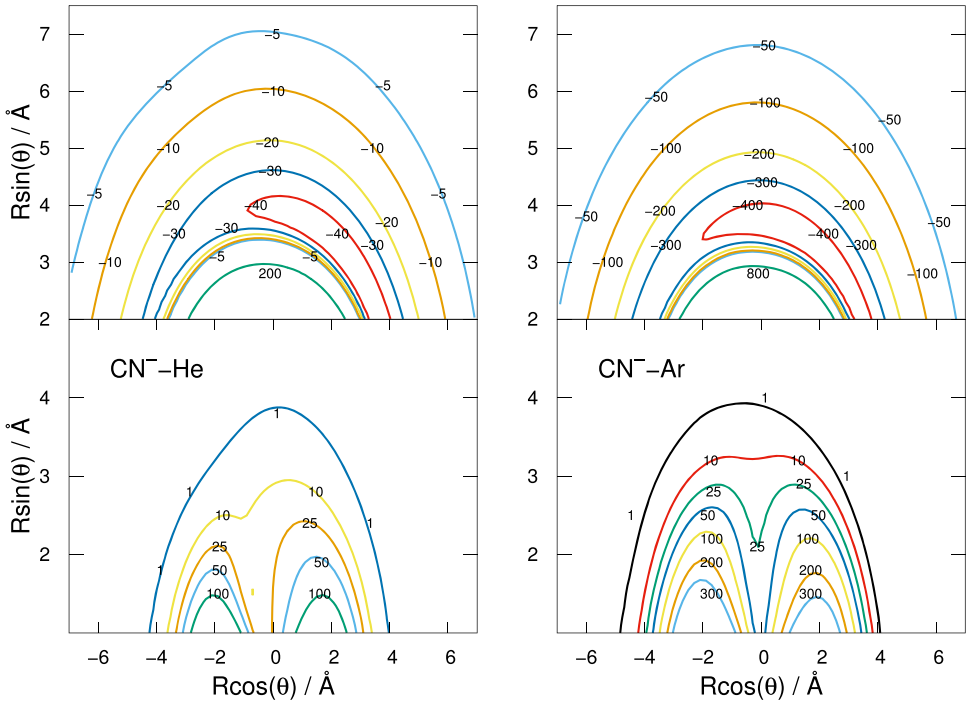

FIG. 2. Contour plots for $CN^-(^1\Sigma^+)$/He (left) and $CN^-(^1\Sigma^+)$/Ar (right) of vibrationally averaged matrix elements $V_{0,0}(R, \theta)$ (top) and $V_{0,1}(R, \theta)$ (bottom) projected onto Cartesian coordinates. Energies in cm^{-1}. See the main text for further details.

electrons on the atoms and to the much larger dipole polarizability that dominates the long-range attractive terms with a value of 1.383 a_0^3 for He and 11.070 a_0^3 for Ar.[67]

The off diagonal $V_{0,1}(R, \theta)$ terms, which directly drive vibrationally inelastic $v = 1$ to $v = 0$ transitions, are also shown in Fig. 2. At short distances, the coupling terms are repulsive, becoming negligible rather quickly at longer distances, as is the case for many other atom–diatom systems, where the vibrational coupling features are largely short-range coupling regions. The interaction of CN^- with Ar is more repulsive at a close range and for a broader range of geometries than is the case for He. These findings suggest already that low-energy collisions with Ar will be likely to induce larger vibrational cross sections than for the same collisions involving He atoms. Such expected behavior will be in fact confirmed below by our actual calculations.

The PESs for CN^-/He and CN^-/Ar can be compared to similar systems such as C_2^-/He and C_2^-/Ar that we have recently investigated.[21] The location of the minimum interaction energy for both anions interacting with He and Ar, respectively, is very similar with the main difference being the perpendicular angle of the well for C_2^-. The off-diagonal matrix elements for these systems are also similar in magnitude and range, but being slightly larger for the interaction of He and Ar with C_2^-, explaining the larger quenching rates for this anion (see below). The PES for the corresponding neutral systems CN/He and CN/Ar, which were reported by Saidani *et al.*, can also be compared.[68] In this case, the well depth for He interacting with both CN and CN^- is similar, but for Ar, the interaction with the anion is somewhat weaker. As expected, the interaction potential for He and Ar interacting with the anion extends further than the corresponding neutral systems. The off-diagonal elements for the neutral and anionic systems are broadly similar.

The coupled-channel (CC) scattering calculations to be discussed in Sec. IV require the vibrationally averaged matrix elements in the form of the familiar multipole expansion given as

$$V_{v,v'}(R,\theta) = \sum_{\lambda}^{\lambda_{\max}} V_{v,v'}^{\lambda}(R) P_{\lambda}(\cos\theta). \tag{4}$$

Figure 3 shows the multipole expansion coefficients for the first three $V_{0,0}(R, \theta)$ terms for both systems. As anticipated from the broad spatial similarity of the contour plots, the multipole expansion for the vibrationally averaged matrix elements is very close to that obtained from considering the anion as a rigid rotor. This justifies our previous treatment of purely rotationally inelastic transitions where we considered the anion to behave as a rigid rotor (RR),[33,35] and we refer the reader to these works for a discussion of pure rotational transitions.

It is also worthy to note about the diagonal coupling matrix elements reported in Fig. 3 on how the much more polarizable Ar projectile gives the three lowest multipolar terms as attractive contributions to the interaction, thereby indicating that their collective effects during the interaction would be to draw the heavier partner closer to the anion. On the other hand, the same three coefficients for the lighter He partner (the left-hand panel in Fig. 3) exhibit much shallower attractive wells and only for two of the coefficients, with

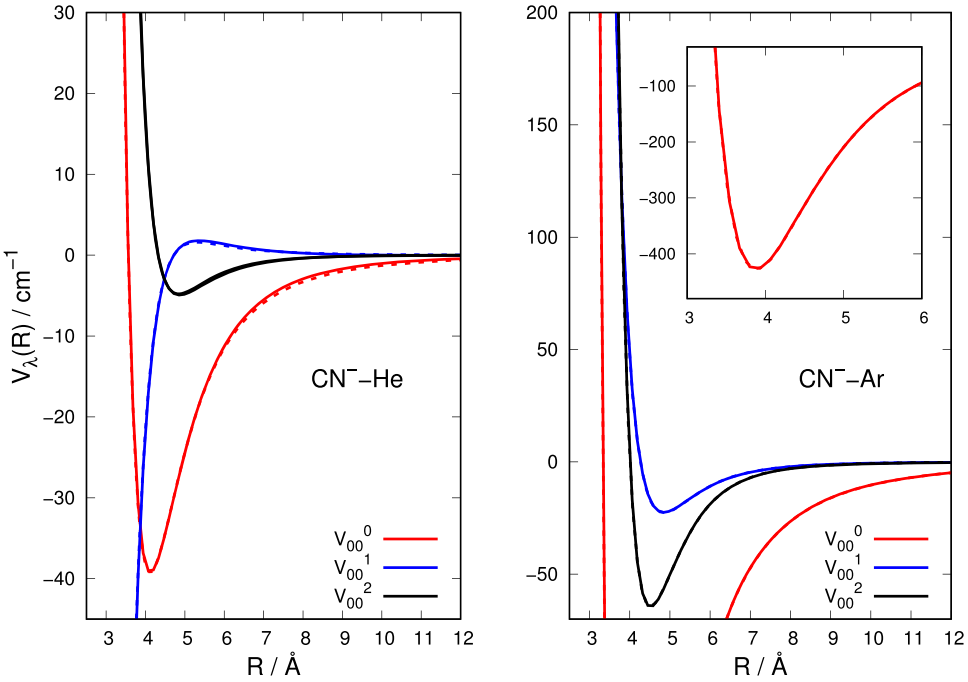

FIG. 3. $V^{\lambda}_{0,0}(R)$ expansion coefficients for λ = 0, 1, and 2 terms for CN^-/He (left) and CN^-/Ar (right). The rigid rotor (RR) values are also plotted as dashed lines but essentially overlap the vibrationally averaged coefficients discussed in the present work.

the $\lambda = 1$ coefficient showing instead a slightly repulsive behavior at intermediate distances.

The off-diagonal expansion coefficients $V^{\lambda}_{0,1}$ are shown in Fig. 4. All terms quickly approach zero as R is increased. For both systems, the $V^{\lambda}_{0,1}(R)$ coefficients are mostly steeply repulsive as R decreases. As expected from the contour plots, the $V^{\lambda}_{0,1}(R)$ terms are found to be much more repulsive for the CN^-/Ar interaction, with their turning points located at larger distances than those for the He partner.

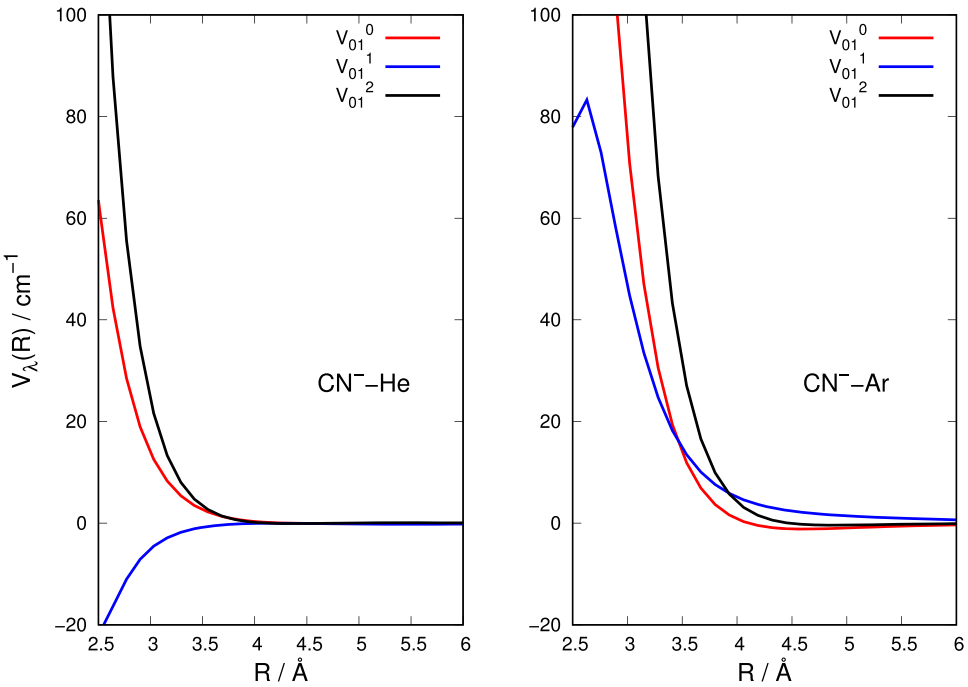

FIG. 4. $V^{\lambda}_{1,0}(R)$ expansion coefficients for λ = 0, 1, and 2 terms for CN^-/He (left) and CN^-/Ar (right).

Such features of the interactions again suggest a larger dynamical vibrational inelasticity for the case of Ar atoms than for the He collision partners.

IV. QUANTUM SCATTERING CALCULATIONS

Quantum scattering calculations were carried out using the coupled channel (CC) method to solve the Schrödinger equation for a scattering of an atom with a diatomic molecule as implemented in our in-house code, ASPIN.[69] The method has been described in detail many times before, from one of its earliest, now classic formulations[70] to one of its more recent, computation-oriented visitation from our own work.[69] Therefore, only a summary of the method will be given here with all equations given in atomic units. By starting with the form employed for any given total angular momentum $\mathbf{J} = \mathbf{l} + \mathbf{j}$, the scattering wavefunction is expanded as

$$\Psi^{JM}(R, r, \Theta) = \frac{1}{R}\sum_{v,j,l} f^{J}_{vlj}(R)\chi_{v,j}(r)\mathscr{Y}^{JM}_{jl}(\hat{\mathbf{R}}, \hat{\mathbf{r}}), \tag{5}$$

where l and j are the orbital and rotational angular momentum, respectively, and $\mathscr{Y}^{JM}_{jl}(\hat{\mathbf{R}}, \hat{\mathbf{r}})$ are coupled-spherical harmonics for l and j, which are eigenfunctions of J. $\chi_{v,j}(r)$ are the radial part of the rovibrational eigenfunctions of the molecule. The values of l and j are constrained, via Clebsch–Gordan coefficients, such that their final summation is compatible with the specific total angular momentum J that is considered.[69,70] $f^{J}_{vlj}(R)$ are the radial expansion functions, which need to be determined from the propagation of the radial coupled equations.

Substituting the expansion into the Schrödinger equation with the Hamiltonian for atom–diatom scattering as defined in detail in Refs. 69 and 70 leads to the CC equations for each contributing J,

$$\left(\frac{d^2}{dR^2} + \mathbf{K}^2 - \mathbf{V} - \frac{\mathbf{l}^2}{R^2}\right)\mathbf{f}^{J} = 0. \tag{6}$$

Here, each element of $\mathbf{K} = \delta_{i,j} 2\,\mu(E - \varepsilon_i)$ (where ε_i is the channel asymptotic energy), μ is the reduced mass of the system, $\mathbf{V} = 2\,\mu\mathbf{U}$ is the interaction potential matrix between channels, and $\mathbf{l}^2$ is the matrix of the orbital angular momentum. For the rovibrational scattering calculations of interest in the present study, the matrix elements $\mathbf{U}$ are given explicitly as

$$\langle vjlJ|V|v'j'l'J\rangle = \int_0^\infty \mathrm{d}r \int \mathrm{d}\hat{\mathbf{r}} \int \mathrm{d}\hat{\mathbf{R}}\, \chi_{v,j}(r)\mathscr{Y}^{JM}_{jl}(\hat{\mathbf{R}}, \hat{\mathbf{r}})^* \times |V(R, r, \theta)|\chi_{v',j'}(r)\mathscr{Y}^{JM}_{j'l'}(\hat{\mathbf{R}}, \hat{\mathbf{r}}). \tag{7}$$

Since the intermolecular potential $V(R, r, \theta)$ is expressed as in Eq. (4), then Eq. (7) can be written as

$$\langle vjlJ|V|v'j'l'J\rangle = \sum_{\lambda=0}^{\infty} V^{\lambda}_{v,v'}(R) f^{J}_{\lambda jlj'l'}, \tag{8}$$

where the $f^{J}_{\lambda jlj'l'}$ terms are the Percival-Seaton coefficients

$$f^{J}_{\lambda jlj'l'} = \int \mathrm{d}\hat{\mathbf{r}} \int \mathrm{d}\hat{\mathbf{R}}\quad \mathscr{Y}^{JM}_{jl}(\hat{\mathbf{R}}, \hat{\mathbf{r}})^* P_\lambda(\cos\theta)\mathscr{Y}^{JM}_{j'l'}(\hat{\mathbf{R}}, \hat{\mathbf{r}}), \tag{9}$$

for which analytical forms are known.[69] Equation (8) also makes use of the widely known approximation

$$V^{\lambda}_{v,v'}(R) \approx V^{\lambda}_{vjv'j'}(R) \tag{10}$$

for all j such that the effect of rotation on the vibrational matrix elements is ignored for reasons that shall be further discussed below.

The CC equations are propagated outwards from the classically forbidden region to a sufficient distance where the scattering matrix $\mathbf{S}$ can be obtained. The inelastic rovibrational state-changing cross sections are obtained as

$$\sigma_{vj\to v'j'} = \frac{\pi}{(2j+1)k^2_{vj}}\sum_J (2J+1)\sum_{l,l'} |\delta_{vlj,v'l'j'} - S^{J}_{vlj,v'l'j'}|^2. \tag{11}$$

To converge the CC equations, a rotational basis set was also used: for both systems, it included up to $j = 20$ rotational functions for each vibrational state. The CC equations were propagated between 1.7 Å and 100.0 Å using the log-derivative propagator[71] up to 60 Å and the variable-phase method at larger distances.[72] The potential energy was interpolated between calculated $V^{\lambda}_{v,v'}(R)$ values using a cubic spline. For $R < 2.5$ Å, the $V^{\lambda}_{v,v'}(R)$ were extrapolated as $\frac{a_\lambda}{R} + b_\lambda R$, while for $R > 20$ Å, the $\lambda = 0$ terms were extrapolated as $\frac{c}{R^4} + \frac{d}{R^6}$. As our *ab initio* calculated interaction energies were computed to $R = 25$ Å, where the interaction energy is negligible for the temperatures of interest here, the extrapolated form has also a negligible effect on cross sections.[73]

A number of parameters of the calculation were checked for convergence. The scattering cross sections differed by around 10%–15% on going from 10 to 19 λ terms. This is less precise than for rotationally inelastic cross sections where convergence to around 1% is typical and is due to the very small cross sections for these processes, which makes obtaining precise and stable values more difficult to achieve. For production calculations, 10 λ terms were included for each $V_{v,v'}(R)$ as a compromise between accuracy and computational time. The effect of the vibrational basis set was also considered. It was found that, for the $v = 1$ and $v = 2$ levels, which are the states of interest here (see Sec. V), it was sufficient to only include these states. Including the $v = 3$ state had a negligible effect on the $v = 1$ and $v = 2$ quenching cross sections. The rotational $j = 20$ basis gave convergence to better than 1% for CN^-/He, while for CN^-/Ar, convergence to about 10% was achieved.

Scattering calculations were carried out for collision energies between 1 cm^{-1} and 1000 cm^{-1} using steps of 0.1 cm^{-1} for energies up to 100 cm^{-1}, 0.2 cm^{-1} for 100–300 cm^{-1}, 1.0 cm^{-1} for 300 cm^{-1}–500 cm^{-1}, and 10.0 cm^{-1} for 500 cm^{-1}–1000 cm^{-1}. This energy grid was used to ensure that important features such as resonances appearing in the cross sections were accounted for and their contributions included when the corresponding rates were calculated. At low collision energies, the positions and widths of such resonances will be very sensitive to the details of the PES.

For CN^-/Ar, the number of partial waves was increased with increasing energy as usual, requiring $J = 120$ for the highest energies considered. For the CN^-/He system, however, inverse behavior was encountered: at low scattering energies below 100 cm^{-1}, more partial waves were required (up to $J = 80$) to converge the vibrationally inelastic partial cross sections than at higher energies where only up to $J = 35$ was required. We suspect this is due to the very small cross sections so that at low energies it becomes difficult to converge the calculations as all partial waves contribute uniformly very small values. Hence, many more of them need inclusion for acceptable convergent behavior to occur.

Vibrationally inelastic cross sections were computed for the $v = 1$ and $v = 2$ states of CN^- for collisions with He. Due to time and memory constraints, only $v = 1$ states of CN^- were considered for Ar collisions. We think, however, that such calculations are already sufficient for our results to make convincingly our main points, as discussed further below.

V. VIBRATIONALLY INELASTIC CROSS SECTIONS AND RATE COEFFICIENTS

Figure 5 compares vibrationally inelastic rotationally elastic (for $j = j' = 0$) cross sections for the de-excitation $v = 1 \rightarrow v = 0$, $v = 2 \rightarrow v = 1$, and $v = 2 \rightarrow v = 0$ transitions for CN^- colliding with He and $v = 1 \rightarrow v = 0$ for CN^-/Ar. At low collision energies below 100 cm^{-1}, the cross sections for He are very small, which are orders of magnitude less than rotationally inelastic collisions for this system.[33] The cross sections show resonances at lower collision energies due to the shape and/or Feshbach resonances. As expected, due to the larger energy difference, the $v = 2 \rightarrow v = 0$ process is smaller than the $v = 2 \rightarrow v = 1$ and $v = 1 \rightarrow v = 0$ cross sections. At collision energies above 100 cm^{-1}, the cross sections rapidly increase in value, a behavior typically observed also in other systems for vibrationally inelastic cross sections.[11–14]

The CN^-/Ar cross sections are found to be about four orders of magnitude larger than those we have obtained for He at lower energies, also showing many distinct resonance features, which are brought about by the presence of a stronger interaction with the molecular anion. The detailed analysis of such a forest of resonances would also be interesting and perhaps would be warranted in the case of existing experimental data on such processes, of which we are not aware until now, but would require a substantial extension of the present work. Thus, we do not intend to carry it out now, being somewhat outside the main scope of the present study, and are leaving it for future extension of this study in our laboratory.

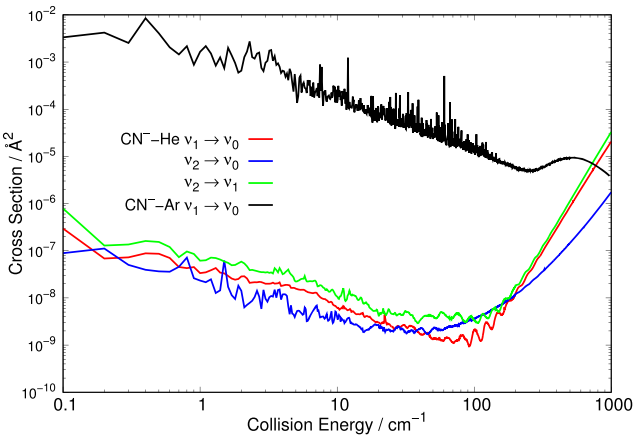

FIG. 5. Scattering cross sections for vibrationally inelastic collisions of CN^- with He and Ar.

The far larger cross sections we found for the Ar projectile are a consequence of the deeper attractive well for the $V_{v,v}(R, \theta)$ diagonal matrix elements and the larger off-diagonal $V_{v,v'}(R, \theta)$ matrix elements (see Fig. 2), i.e., they stem from distinct differences in the strengths of the coupling potential terms that drive the inelastic dynamics for the Ar collision partner.

The general features of the vibrationally inelastic cross sections shown in Fig. 5 are indeed similar to those which we have obtained earlier for the C_2^- anion colliding with the He, Ne, and Ar set of systems that we have recently studied.[21] For both the anions, we have found that the vibrational quenching cross sections with He are uniformly very small, while we also found that they increase by orders of magnitude when the larger and more polarizable Ar atom becomes the collisional partner for either of these anionic molecules. Although such general behavior could be reasonably expected from what we know in these systems about their interaction forces, it is nevertheless reassuring to obtain quantitative confirmation on the extent of the size differences from detailed, and in principle exact, scattering calculations.

The computed inelastic cross sections of Sec. IV can in turn be used to obtain the corresponding thermal rate constants over ranges of temperature of interest for placing the present anion in cold environments. The corresponding $k_{v \rightarrow v'}(T)$ can be evaluated, in fact, as the convolution of the computed inelastic cross sections over a Boltzmann distribution of the relative collision energies of the interacting partners as

$$k_{v \rightarrow v'}(T) = \left(\frac{8}{\pi \mu k_B^3 T^3}\right)^{1/2} \int_0^\infty E_c \sigma_{v \rightarrow v'}(E_c) e^{-E_c/k_B T} dE_c, \qquad (12)$$

where $E_c = \mu v^2/2$ is the kinetic energy in the collision calculations. The rate constants were computed between 5 K and 100 K in 1 K intervals. Figure 6 shows the rates for vibrationally inelastic rotationally elastic ($j = j' = 0$) transitions corresponding to the cross sections in Fig. 5. The figure also shows rates for the corresponding transitions of the similar C_2^-/He and Ar systems. For CN^-/He, the rate constants for vibrational quenching are very small, even lower than those for C_2^-/He and around nine orders of magnitude lower than those for CN^-/He rotationally inelastic collisions.[33] For CN^-/Ar, the $v = 1 \rightarrow v = 0$ rate constants are about four orders of magnitude larger than those for He but about three orders of magnitude less than those for the corresponding transition for C_2^-/Ar. The $v = 2 \rightarrow v = 1$ rate constants for CN^-/He is broadly similar to those for $v = 1 \rightarrow v = 0$, while as expected the $v = 2 \rightarrow v = 0$ rate constants are slightly smaller.

The increase in rate constant sizes on going from He to Ar vibrational collisions is similar to what was found for rotationally

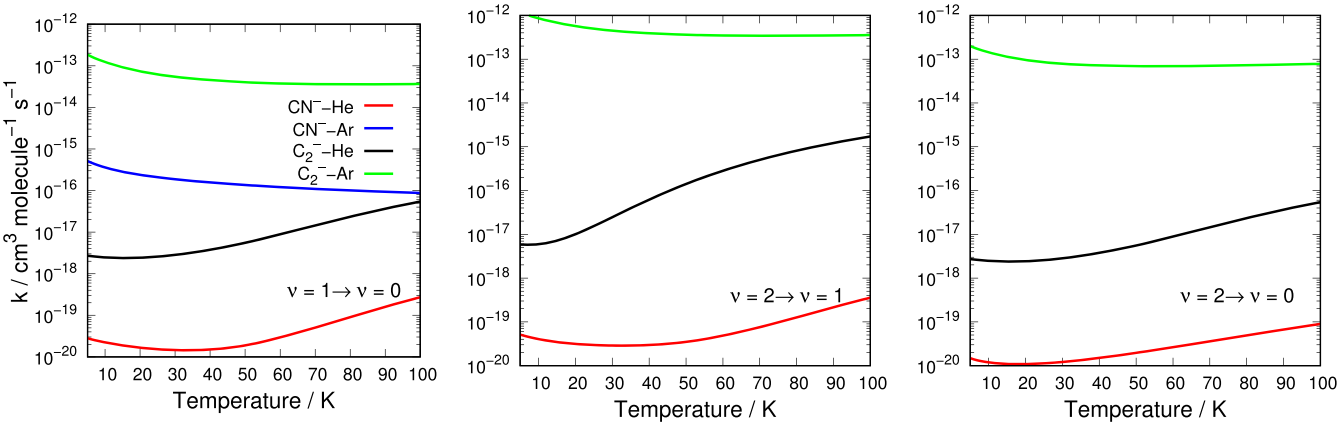

FIG. 6. Rate constants $k_{v\to v'}(T)$ for vibrationally inelastic transitions in CN^-/He and Ar collisions. Also shown are the corresponding values for C_2^-/He and Ar.[21]

inelastic collisions for CN^-[35] and C_2^-[74], and, as shown in Fig. 6, vibrationally inelastic collisions for C_2^-.[21] This trend, while seemingly to be expected with the stronger interaction potential for the larger atom, is not easy to predict *a priori*. Kato *et al.* and Ferguson measured vibrational quenching rates for N_2^+ in collisions with He, Ne, Ar, Xe, and Kr atoms[75] and O_2^+ with He, Ne, and Ar atoms,[76] respectively, at 300 K. For both cations, quenching rates increased with the size of the atom, suggesting that the polarizability of the colliding atom plays an important role. In contrast, Saidani *et al.* calculated the quenching rates for CN with He and Ar over a wide range of temperatures and found that the cross sections and rates for Ar were orders of magnitude lower than those for He.[68] However, ionic interactions are driven by different forces than those acting between neutrals, so it is not obvious how such a result relates to the present findings for an anion. Analytical models can also be used to gain insight into vibrational quenching such as the work of Dashevskaya *et al.*, where the quenching rate for $v = 1 \to v = 0$ for N_2/He was calculated over a large range of temperatures from 70 K to 3000 K.[77] The rates obtained were in good agreement with the experiment and similar to those found here for CN^-/He at 100 K. It would be interesting to apply these models to the anion–neutral collisions we have studied here.

The work we have presented here and the similar findings from our previous study[21] on a different diatomic anion like C_2^- strongly suggest that the process of vibrational inelasticity in multiply bonded anionic molecules by low-T collisions with neutral noble gases is rather inefficient. The rates for quenching found here are even smaller than those we had found earlier for C_2^-, also uniformly smaller than those known for many neutral diatomic molecules and cations.[21]

The quenching rates and Einstein A coefficients, which we have mentioned and shown earlier in this work, can be used to consider the properties of the critical density $n^i_{\rm crit}(T)$ for CN^- vibrations, which is given as

$$n^i_{\rm crit}(T) = \frac{A_{ij}}{\sum_{j\neq i} k_{ij}(T)}. \tag{13}$$

This quantity gives the gas density values that would be required so that collisional state-changing processes match in size with those which lead to collision-less emission via spontaneous decay. It is used in astronomical contexts to assess the possible densities required for the local thermal equilibrium (LTE) to be reached and are usually applied for rotational transitions in molecules that can occur in the interstellar medium (ISM).

In the present case of CN^-/He, when we apply Eq. (13) to the $v = 1$ and $v = 2$ vibrational state-changing process, it gives $n^i_{\rm crit}(T) \approx 10^{19}$ cm^{-3}–10^{20} cm^{-3} at 100 K. Current kinetics models, which describe the density conditions in molecular clouds, indicate a wide variety of densities being present: from diffuse molecular clouds estimated at around 10^2 cm^{-3} to dense molecular clouds that are considered to be between 10^3 cm^{-3} and 10^6 cm^{-3}.[78,79] The critical density obtained here for the vibrational decay of CN^- interacting with environmental He atoms was found to be orders of magnitude larger than those expected in the ISM regions where CN^- has been detected, clearly suggesting that thermal equilibrium for these processes will likely never be attained and that the presently computed radiative transitions determine that CN^- populates essentially only the ground vibrational level in the ISM.

VI. CONCLUSIONS

The cross sections and corresponding rate constants for vibrationally inelastic transitions of CN^- colliding with He and Ar atoms have been calculated using new *ab initio* potential energy surfaces. As for atom–diatom vibrationally inelastic collisions, the rate constants for both CN^-/He and CN^-/Ar are very small, even smaller than the corresponding values of the similar C_2^-/He and C_2^-/Ar systems. Although more work is required before definitive conclusions can be drawn, it appears from the present calculations that vibrationally inelastic collisions of molecular anions with neutral atoms (or at least noble gas atoms) are similar to neutral molecule–atom collisions in which they generate similarly small transition probabilities and their collision mechanisms for transferring relative energy,

at sub-thermal and thermal conditions, to the vibrational internal motion of the anion is rather inefficient. This is in contrast with the generally more efficient collisional energy transfer probabilities, which are found for molecular cation–atom systems in the current literature.[21]

For the anion of interest here, this is not a crucial concern when wanting to find alternative paths that are more efficient in cooling its internal vibrational motion, since CN^- can dissipate energy through spontaneous dipole emission (Sec. II). On the other hand, in the case of homonuclear anions such as C_2^- (of current interest for laser cooling cycles in cold traps[22]), where this process is forbidden, collisions are likely to be the primary means for quenching its vibrational motion. In such cases, high gas pressures and the use of larger noble buffer gasses seem to be required.

The present calculations confirm that collisional energy transfer paths, which involve vibrational degrees of freedom for a molecular anion under cold trap conditions, are invariably very inefficient and are several orders of magnitude smaller than the collisional energy-changing paths, which involve their rotational degrees of freedom. One can, therefore, safely estimate that these two paths to energy losses are markedly decoupled with one another and can be treated on a separate footing within any kinetics modeling of their behavior.

SUPPLEMENTARY MATERIAL

See the supplementary material for the multipolar coefficients for the Legendre expansion of the new vibrational PESs for CN^-/He and CN^-/Ar provided via Fortran program routines, as well as the coupling coefficients for the vibrational dynamics. Subroutines for the inelastic and elastic rate coefficients for the two systems studied in the present paper are also presented.

ACKNOWLEDGMENTS

We acknowledge the financial support of the Austrian FWF agency through research Grant No. P29558-N36. L.G.-S. is thankful to MINECO (Spain) for Grant No. PGC2018-09644-B-100.

DATA AVAILABILITY

Fortran programs and subroutines for the CN^-/He and CN^-/Ar PESs used are available in the supplementary material along with the vibrational coupling coefficients and vibrational quenching rate constants.

REFERENCES

[1] K. Takayanagi, "Vibrational and rotational transitions in molecular collisions," Prog. Theor. Phys. Suppl. **25**, 1–98 (1963).
[2] D. Secrest, "Theory of rotational and vibrational energy transfer in molecules," Annu. Rev. Phys. Chem. **24**, 379–406 (1973).
[3] D. J. Krajnovich, C. S. Parmenter, and D. L. Catlett, "State-to-state vibrational transfer in atom-molecule collisions. Beams vs. bulbs," Chem. Rev. **87**, 237–288 (1987).
[4] D. Secrest and B. R. Johnson, "Exact quantum mechanical calculation of a collinear collision of a particle with a harmonic oscillator," J. Chem. Phys. **45**, 4556 (1966).
[5] W. Eastes and D. Secrest, "Calculation of rotational and vibrational transitions for the collision of an atom with a rotating vibrating diatomic oscillator," J. Chem. Phys. **56**, 640 (1972).
[6] W. C. Campbell, G. C. Groenenboom, H.-I. Lu, E. Tsikata, and J. M. Doyle, "Time-domain measurements of spontaneous vibrational decay of magnetically trapped NH," Phys. Rev. Lett. **100**, 083003 (2008).
[7] I. Kozyryev, L. Baum, K. Matsuda, P. Olson, B. Hemmerling, and J. M. Doyle, "Collisional relaxation of vibrational states of SrOH with He at 2 K," New J. Phys. **17**, 045003 (2015).
[8] D. Caruso, M. Tacconi, F. A. Gianturco, and E. Yurtsever, "Quenching vibrations by collisions in cold traps: A quantum study for $MgH^+(X^1\Sigma^+)$ with ^4He (^1S)," J. Chem. Sci. **124**, 93 (2012).
[9] W. Rellergent, S. T. Sulliven, S. J. Schowalter, S. Kotochigova, K. Chen, and E. R. Hudson, "Evidence for sympathetic vibrational cooling of translationally cold molecules," Nature **495**, 490 (2013).
[10] F. F. S. van der Tak, F. Lique, A. Faure, J. H. Black, and E. W. van Dishoeck, "The Leiden atomic and molecular database (LAMDA): Current status, recent updates, and future plans," Atoms **8**, 15 (2020).
[11] C. Balança and F. Dayou, "Ro-vibrational excitation of SiO by collision with helium at high temperature," Mon. Not. R. Astron. Soc. **469**, 1673 (2017).
[12] R. Toboła, F. Lique, J. Kłos, and G. Chałasiński, "Ro-vibrational excitation of SiS by He," J. Phys. B: At., Mol. Opt. Phys. **41**, 155702 (2008).
[13] F. Lique and A. Spielfiedel, "Ro-vibrational excitation of CS by He," Astron. Astrophys. **462**, 1179 (2007).
[14] F. Lique, A. Spielfiedel, G. Dhont, and N. Feautrier, "Ro-vibrational excitation of the SO molecule by collision with the He atom," Astron. Astrophys. **458**, 331 (2006).
[15] T. Stoecklin, P. Halvick, M. A. Gannounim, M. Hochlaf, S. Kotochigova, and E. R. Hudson, "Explanation of efficient quenching of molecular ion vibrational motion by ultracold atoms," Nat. Commun. **7**, 11234 (2016).
[16] B. Yang, X. H. Wang, P. C. Stancil, J. M. Bowman, N. Balakrishnan, and R. C. Forrey, "Full-dimensional quantum dynamics of rovibrationally inelastic scattering between CN and H_2," J. Chem. Phys. **145**, 224307 (2016).
[17] Y. Kalugina, F. Lique, and S. Marinakis, "New *ab initio* potential energy surfaces for the ro-vibrational excitation of $OH(X^2\Pi)$ by He," Phys. Chem. Chem. Phys. **16**, 13500 (2014).
[18] I. Iskandarov, F. A. Gianturco, M. Hernández Vera, R. Wester, H. da Silva, Jr., and O. Dulieu, "Shape and strength of dynamical couplings between vibrational levels of the H_2^+, HD^+ and D_2^+ molecular ions in collision with He as a buffer gas," Eur. Phys. J. D **71**, 141 (2017).
[19] T. Stoecklin and A. Voronin, "Vibrational and rotational cooling of NO^+ in collisions with He," J. Chem. Phys. **134**, 204312 (2011).
[20] T. Stoecklin and A. Voronin, "Vibrational and rotational energy transfer of CH^+ in collisions with ^4He and ^3He," Eur. Phys. J. D **46**, 259 (2008).
[21] B. P. Mant, F. A. Gianturco, R. Wester, E. Yurtsever, and L. González-Sánchez, "Ro-vibrational quenching of C_2^- anions in collisions with He, Ne and Ar atoms," Phys. Rev. A **102**, 062810 (2020).
[22] P. Yzombard, M. Hamamda, S. Gerber, M. Doser, and D. Comparat, "Laser cooling of molecular anions," Phys. Rev. Lett. **114**, 213001 (2015).
[23] S. E. Bradforth, E. H. Kim, D. W. Arnold, and D. M. Neumark, "Photoelectron spectroscopy of CN^-, NCO^-, and NCS^-," J. Chem. Phys. **98**, 800 (1993).
[24] D. Forney, W. E. Thompson, and M. E. Jacox, "The vibrational spectra of molecular ions isolated in solid neon. IX. HCN^+, HNC^+, and CN^-," J. Chem. Phys. **97**, 1664 (1992).
[25] C. A. Gottlieb, S. Brünken, M. C. McCarthy, and P. Thaddeus, "The rotational spectrum of CN^-," J. Chem. Phys. **126**, 191101 (2007).
[26] P. Botschwina, "Spectroscopic properties of the cyanide ion calculated by SCEP CEPA," Chem. Phys. Lett. **114**, 58–62 (1985).
[27] K. A. Peterson and R. C. Woods, "An *ab initio* investigation of the spectroscopic properties of BCl, CS, CCl^+, BF, CO, CF^+, N_2, CN^-, and NO^+," J. Chem. Phys. **87**, 4409 (1987).

[28]T. J. Lee and C. E. Dateo, "Accurate spectroscopic characterization of $^{12}C^{14}N^-$, $^{13}C^{14}N^-$, $^{12}C^{15}N^-$," Spectrochim. Acta, Part A **55**, 739 (1999).
[29]J. Berkowitz, W. A. Chupka, and T. A. Walter, "Photo ionization of HCN: The electron affinity and heat of formation of CN," J. Chem. Phys. **50**, 1497 (1969).
[30]R. Klein, R. P. McGinnis, and S. R. Leone, "Photodetachment threshold of CN^- by laser optogalvanic spectroscopy," Chem. Phys. Lett. **100**, 475 (1983).
[31]M. Simpson, M. Nötzold, A. Schmidt-May, T. Michaelsen, B. Bastian, J. Meyer, R. Wild, F. A. Gianturco, M. Milovanović, V. Kokoouline, and R. Wester, "Threshold photodetachment spectroscopy of the astrochemical anion CN^-," J. Chem. Phys. **153**, 184309 (2020).
[32]M. Agúndez, J. Cernicharo, M. Guélin, C. Kahane, E. Roueff, J. Kłos, F. J. Aoiz, F. Lique, N. Marcelino, J. R. Goicoechea, M. González García, C. A. Gottlieb, M. C. McCarthy, and P. Thaddeus, "Astronomical identification of CN^-, the smallest observed molecular anion," Astron. Astrophys. **517**, L2 (2010).
[33]L. González-Sánchez, B. P. Mant, R. Wester, and F. A. Gianturco, "Rotationally inelastic collisions of CN^- with He: Computing cross sections and rates in the interstellar medium," Astrophys. J. **897**, 75 (2020).
[34]J. Kłos and F. Lique, "First rate coefficients for an interstellar anion: Application to the CN^--H_2 collisional system," Mon. Not. R. Astron. Soc. **418**, 271–275 (2011).
[35]L. González-Sánchez, E. Yurtsever, B. P. Mant, R. Wester, and F. A. Gianturco, "Collision-driven state-changing efficiency of different buffer gases in cold traps: He(^1S), Ar (^1S) and p-H_2($^1\Sigma$) on trapped CN^-($^1\Sigma$)," Phys. Chem. Chem. Phys. (published online) (2020).
[36]S. Petrie, "Novel pathways to CN^- within interstellar clouds and circumstellar envelopes: Implications for IS and CS chemistry," Mon. Not. R. Astron. Soc. **281**, 137–144 (1996).
[37]C. Romanzin, E. Louarn, J. Lemaire, J. Žabka, M. Polášek, J.-C. Guillemin, and C. Alcaraz, "An experimental study of the reactivity of CN^- and C_3N^- anions with cyanoacetylene (HC_3N)," Icarus **268**, 242–252 (2016).
[38]S. Jerosimić, F. A. Gianturco, and R. Wester, "Associative detachment (AD) paths for H and CN^- in the gas-phase: Astrophysical implications," Phys. Chem. Chem. Phys. **20**, 5490 (2018).
[39]M. Satta, F. A. Gianturco, F. Carelli, and R. Wester, "A quantum study of the chemical formation of cyano anions in inner cores and diffuse regions of interstellar molecular clouds," Astrophys. J. **799**, 228–235 (2015).
[40]L. Biennier, S. Carles, D. Cordier, J.-C. Guillemin, S. D. Le Picard, and A. Faure, "Low temperature reaction kinetics of CN^- + HC_3N and implications for the growth of anions in titan's atmosphere," Icarus **227**, 123–131 (2014).
[41]A. J. Coates, F. J. Crary, G. R. Lewis, D. T. Young, J. H. Waite, Jr., and E. C. Sittler, Jr., "Discovery of heavy negative ions in Titan's ionosphere," Geophys. Res. Lett. **34**, L22103, https://doi.org/10.1029/2007gl030978 (2007).
[42]V. Vuitton, P. Lavvas, R. V. Yelle, M. Galand, A. Wellbrock, G. R. Lewis, A. J. Coates, and J.-E. Wahlund, "Negative ion chemistry in Titan's upper atmosphere," Planet. Space Sci. **57**, 1558–1572 (2009).
[43]A. McKellar, "Evidence for the molecular origin of some hitherto unidentified interstellar lines," Publ. Astron. Soc. Pac. **52**, 187 (1940).
[44]H. Burton, R. Mysliwiec, R. C. Forrey, B. H. Yang, P. C. Stancil, and N. Balakrishnan, "Fine-structure resolved rotational transitions and database for CN + H_2 collisions," Mol. Astrophys. **11**, 23–32 (2018).
[45]F. Lique, A. Spielfiedel, N. Feautrier, I. F. Schneider, J. Kłos, and M. H. Alexander, "Rotational excitation of CN($X^2\Sigma^+$) by He: Theory and comparison with experiments," J. Chem. Phys. **132**, 024303 (2010).
[46]F. Lique and J. Kłos, "Hyperfine excitation of CN by He," Mon. Not. R. Astron. Soc. **413**, L20–L23 (2011).
[47]Y. Kalugina, F. Lique, and J. Kłos, "Hyperfine collisional rate coefficients of CN with H_2($j = 0$)," Mon. Not. R. Astron. Soc. **422**, 812 (2012).
[48]Y. Kalugina, J. Kłos, and F. Lique, "Collisional excitation of CN($X^2\Sigma^+$) by para- and ortho-H_2: Fine-structure resolved transitions," J. Chem. Phys. **139**, 074301 (2013).
[49]Y. Kalugina and F. Lique, "Hyperfine excitation of CN by para- and ortho-H_2," Mon. Not. R. Astron. Soc. **446**, L21–L25 (2015).
[50]J. L. Doménech, O. Asvany, C. R. Markus, S. Schlemmer, and S. Thorwirth, "High-resolution infrared action spectroscopy of the fundamental vibrational band of CN^+," J. Mol. Spectrosc. **374**, 111375 (2020).
[51]B. Anusuri, "Rotational excitation of cyanogen ion, CN^+ ($X^1\Sigma^+$) by He collisions," Comput. Theor. Chem. **1176**, 112748 (2020).
[52]H.-J. Werner, P. J. Knowles, G. Knizia, F. R. Manby, and M. Schütz, "Molpro: A general-purpose quantum chemistry program package," Wiley Interdiscip. Rev.: Comput. Mol. Sci. **2**, 242–253 (2012).
[53]H.-J. Werner, P. J. Knowles, G. Knizia, F. R. Manby, M. Schütz *et al.*, Molpro, version 2019.2, a package of *ab initio* programs, 2019, see https://www.molpro.net.
[54]C. Hampel, K. A. Peterson, and H.-J. Werner, "A comparison of the efficiency and accuracy of the quadratic configuration interaction (QCISD), coupled cluster (CCSD), and Brueckner coupled cluster (BCCD) methods," Chem. Phys. Lett. **190**, 1–12 (1992).
[55]M. J. O. Deega and P. J. Knowles, "Perturbative corrections to account for triple excitations in closed and open shell coupled cluster theories," Chem. Phys. Lett. **227**, 321–326 (1994).
[56]D. E. Woon and T. H. Dunning, Jr., "Gaussian basis sets for use in correlated molecular calculations. III. The atoms aluminum through argon," J. Chem. Phys. **98**, 1358 (1993).
[57]D. E. Woon and T. H. Dunning, Jr., "Gaussian basis sets for use in correlated molecular calculations. IV. Calculation of static electrical response properties," J. Chem. Phys. **100**, 2975 (1994).
[58]R. J. Le Roy, "LEVEL: A computer program for solving the radial Schrödinger equation for bound and quasibound levels," J. Quant. Spectrosc. Radiat. Transfer **186**, 167 (2017).
[59]J. S. A. Brooke, R. S. Ram, C. M. Western, G. Li, D. W. Schwenke, and P. F. Bernath, "Einstein a coefficients and oscillator strengths for the $A\,^2\Pi$-$X^2\Sigma^+$(red) and $B^2\Sigma^+$-$X^2\Sigma^+$ (violet) systems and rovibrational transitions in the $X^2\Sigma^+$ state of CN," Astrophys. J. **210**, 23 (2014).
[60]H. J. Werner and P. J. Knowles, "A second order multiconfiguration SCF procedure with optimum convergence," J. Chem. Phys. **82**, 5053 (1985).
[61]P. J. Knowles and H.-J. Werner, "An efficient second-order MC SCF method for long configuration expansions," Chem. Phys. Lett. **115**, 259 (1985).
[62]K. R. Shamasundar, G. Knizia, and H.-J. Werner, "A new internally contracted multi-reference configuration interaction method," J. Chem. Phys. **135**, 054101 (2011).
[63]R. A. Kendall, T. H. Dunning, Jr., and R. J. Harrison, "Electron affinities of the first-row atoms revisited. Systematic basis sets and wave functions," J. Chem. Phys. **96**, 6796 (1992).
[64]A. K. Wilson, T. van Mourik, and T. H. Dunning, "Gaussian basis sets for use in correlated molecular calculations. VI. Sextuple zeta correlation consistent basis sets for boron through neon," J. Mol. Struct.: THEOCHEM **388**, 339–349 (1996).
[65]S. F. Boys and F. Bernardi, "Calculation of small molecular interactions by differences of separate total energies - some procedures with reduced errors," Mol. Phys. **19**, 553 (1970).
[66]H. J. Werner, B. Follmeg, and M. H. Alexander, "Adiabatic and diabatic potential energy surfaces for collisions of CN ($X^2\Sigma^+$, $A^2\Pi$) with He," J. Chem. Phys. **89**, 3139 (1988).
[67]C. Gaiser and B. Fellmuth, "Polarizability of helium, neon, and argon: New perspectives for gas metrology," Phys. Rev. Lett. **120**, 123203 (2018).
[68]G. Saidani, Y. Kalugina, A. Gardez, L. Biennier, R. Georges, and F. Lique, "High temperature reaction kinetics of CN($v = 0$) with C_2H_4 and C_2H_6 and vibrational relaxation of CN($v = 1$) with Ar and He," J. Chem. Phys. **138**, 124308 (2013).
[69]D. López-Durán, E. Bodo, and F. A. Gianturco, "ASPIN: An all spin scattering code for atom-molecule rovibrationally inelastic cross sections," Comput. Phys. Commun. **179**, 821 (2008).
[70]A. M. Arthurs and A. Dalgarno, "The theory of scattering by a rigid rotator," Proc. R. Soc. London, Ser. A **256**, 540 (1960).
[71]D. E. Manolopoulos, "An improved log derivative method for inelastic scattering," J. Chem. Phys. **85**, 6425 (1986).
[72]R. Martinazzo, E. Bodo, and F. A. Gianturco, "A modified variable-phase algorithm for multichannel scattering with long-range potentials," Comput. Phys. Commun. **151**, 187 (2003).
[73]B. P. Mant, F. A. Gianturco, L. González-Sánchez, E. Yurtsever, and R. Wester, "Rotationally inelastic processes of C_2^- ($^2\Sigma_g^+$) colliding with He (^{1}S) at low-temperatures: *Ab initio* interaction potential, state-changing rates and kinetic modelling," J. Phys. B: At., Mol. Opt. Phys. **53**, 025201 (2020).

[74]B. P. Mant, F. A. Gianturco, R. Wester, L. González-Sánchez, and E. Yurtsever, "Thermalization of C_2^- with noble gases in cold ion traps," J. Int. Mass Spectrom. **457**, 116426 (2020).
[75]S. Kato, V. M. Bierbaum, and S. R. Leone, "Laser fluorescence and mass spectroscopic measurements of vibrational relaxation of $N_2^+(v)$ with He, Ne, Ar, Kr and Xe," Int. J. Mass Spec. Ion Proc. **149-150**, 469 (1995).
[76]E. E. Ferguson, "Vibrational quench2ing of small molecular ions in neutral collisions," J. Phys. Chem. **90**, 731 (1986).
[77]E. I. Dashevskaya, I. Litvin, E. E. Nikitin, and J. Troe, "Semiclassical extension of the landau-teller theory of collisional energy transfer," J. Chem. Phys. **125**, 154315 (2006).
[78]T. P. Snow and B. J. McCall, "Diffuse atomic and molecular clouds," Annu. Rev. Astron. Astrophys. **44**, 367–414 (2006).
[79]M. Agúndez and J. Cernicharo, "Oxygen chemistry in the circumstellar envelope of the carbon-rich star IRC+10216," Astrophys. J. **650**, 374–393 (2006).